ROLLING PROCESS SIMULATION USING A DEVELOPED EULERIAN FORMULATION

BAYOUMI* H.N.

ABSTRACT

In this paper, an Eulerian formulation is developed from the more general Arbitrary Lagrangian Eulerian (ALE) formulation and is used in rolling process simulation. Starting from the basic principles of continuum mechanics, a consistent ALE formulation is derived. An Eulerian formulation is then obtained by fixing the finite element mesh in space. A finite element program based on the Eulerian formulation has been developed. The program is used to simulate a steady state rolling process. The roll pressure distribution is compared with published experimental results. Comparisons reveal the effectiveness of the developed formulation.

KEYWORDS

Finite element analysis, Eulerian formulation, rolling process.

* Lecturer, Mechanical Design & Production Dept., Cairo University, Giza, Egypt.

INTRODUCTION

Finite element simulations of large strain metal forming processes have been traditionally based on the Lagrangian formulation. In the Lagrangian formulation [1], the finite element mesh, or reference configuration, is attached to the material points of the deforming body. In large strain situations, this can lead to excessive distortion of the finite element mesh and presents a major drawback of the formulation. Distorted meshes reduce the accuracy of numerical integrations and may ultimately result in singular stiffness matrices and computation termination. Another drawback of the Lagrangian approach is the difficulty to model non-material-associated boundary conditions. The fact that boundary conditions have to be specified on the moving material points alters the boundary conditions during the course of deformation. Although remeshing the material domain with a new finite element mesh can remedy the mesh distortion problem, the problem of incorrect representation of boundary conditions will persist between remeshes. In addition, certain approximations have to be introduced to interpolate the material properties for the new mesh from the corresponding old material points. The difficulties in using the pure Lagrangian formulation for metal forming simulation reduce the reliability and accuracy of simulations and often give rise to erroneous fluctuations in predicted forming loads and violation of the plastic incompressibility constraint.

There are some attempts aiming at the adaptation of Eulerian (spatial) formulation, widely used in fluid flow simulations, to large strain and metal forming problems [2]. In the Eulerian description, the finite element mesh is fixed in space. The drawbacks of the Eulerian description are the difficulty to model changing material boundaries and the difficulty to model material-associated boundary conditions. However, the Eulerian description is well-suited for the analysis of metal forming problems of the steady-state type.

The Arbitrary Lagrangian Eulerian (ALE) formulation can alleviate the drawbacks of both the traditional Lagrangian and Eulerian formulations. In the ALE formulation, the finite element mesh need not adhere to the material nor be fixed in space but can move arbitrarily. As the material deforms, the finite element mesh is moved continuously to meet any preset criterion (e.g. optimize elements shape) and the simulation should be completed without user intervention. Since its conception, ALE has been mainly formulated for use in the analysis of fluid flow problems [3]. The ALE technique was also applied in fluid-structure interaction problems to model the fluid domain while the structure domain was handled using the usual Lagrangian description [4]. ALE finite element formulation for the analysis of metal forming problems was later introduced using the operator split technique [5].

An implicit fully coupled ALE formulation specifically designed for large deformation solid mechanics applications was developed by the author [6, 7]. Starting from the basic principles of continuum mechanics, ALE equilibrium equations were derived for both quasi-static and dynamic analyses. A new method for the treatment of convective terms that sidesteps the computation of the spatial gradients of stresses was used in the derivation. Details of the finite element discretization were presented and full expressions for the resulting matrices and vectors were given. The developed formulation was implemented into a 2-D finite element code for elastic-plastic materials. Several quasi-static and dynamic large deformation problems were simulated using the

program. The results showed the effectiveness of the ALE approach in handling contact boundary conditions and in preventing mesh distortion.

In the current work, an Eulerian formulation which is a special case of the general ALE formulation developed in [6] is presented. The paper starts by highlighting the steps involved in the derivation of the fully coupled ALE equations. An Eulerian form of the equilibrium equation is then derived and developed into a 2-D finite element program. The program is used to simulate a steady state strip rolling process. Results are compared with the literature.

GEOMETRIC DESCRIPTION

In the ALE description of motion, the material domain at any time t consists of the set of material particles, whereas the grid domain refers to the set of arbitrary grid points sharing a common boundary with the set of material particles. In Fig. 1, X^m and X^g act as *markers* for a material particle and a grid point that coincide at time t. Let ${}^t x_i^m (X^m, t)$ and ${}^t x_i^g (X^g, t)$ be the vector functions that characterize the motion of the material particle X^m and the grid point X^g respectively. The position of X^m coincident with X^g at time t is given by the value of the functions ${}^t x_i^m$ and ${}^t x_i^g$ as ${}^t x_i$ where, for definiteness, we have distinguished between the value of the function and the functional form. Thus,

$$ {}^t x_i = {}^t x_i^m (X^m, t) = {}^t x_i^g (X^g, t). \tag{1} $$

The material velocity ${}^t v_i$ and the grid point velocity ${}^t v_i^g$ at time t are given by

$$ {}^t v_i = \frac{\partial {}^t x_i^m}{\partial t}\bigg|_{X^m} \tag{2} $$

$$ {}^t v_i^g = \frac{\partial {}^t x_i^g}{\partial t}\bigg|_{X^g}. \tag{3} $$

Throughout the derivation, notations similar to those used by Bathe [8] are adopted. Left superscripts indicate the configuration in which the quantity occurs whereas left subscripts indicate the configuration to which the quantity is referred. Left subscripts may be omitted if the quantity occurs in the same configuration in which it is measured. A quantity with no left superscripts or subscripts indicate an incremental quantity from time t to $t + \Delta t$. The boundary constraint, which ensures that the material domain and the grid domain have the same boundaries at all times, can be expressed as

$$ ({}^t v_i - {}^t v_i^g) {}^t n_i \big|_{\text{on the boundary}} = 0 \tag{4} $$

where ${}^t n_i$ is the unit normal to the boundary surface.

The material derivative of an arbitrary function ${}^t f$ is denoted by a superposed dot and

is defined to be the rate of change of the function holding the material particle X^m fixed

$$^t\dot{f} = \left.\frac{\partial^t f}{\partial t}\right|_{X^m} \tag{5}$$

whereas the time derivative of the function $^t f$ holding the grid point X^g fixed is denoted by a superposed prime

$$^t f' = \left.\frac{\partial^t f}{\partial t}\right|_{X^g}. \tag{6}$$

The relation between the two time derivatives is given by [9]

$$^t\dot{f} = {}^t f' + ({}^t v_i - {}^t v_i^g)\frac{\partial^t f}{\partial^t x_i}. \tag{7}$$

Denoting the incremental material displacements from time t to time $t + \Delta t$ by u_i and the corresponding incremental grid displacements by u_i^g, we have the following relations

$$u_i = {}^t v_i \Delta t \tag{8}$$
$$u_i^g = {}^t v_i^g \Delta t \tag{9}$$
$$^{t+\Delta t} x_i = {}^t x_i + u_i^g \tag{10}$$

where $^{t+\Delta t} x_i$ is the position of the grid point at time $t + \Delta t$.

CONSERVATION OF MASS

The local form of conservation of mass, continuity, at time t is given by

$$^t\dot{\rho} = -{}^t\rho\frac{\partial^t v_i}{\partial^t x_i} \tag{11}$$

where $^t\rho$ is the material density. Using (7), the continuity equation with respect to an arbitrary moving grid point can be expressed as

$$^t\rho' = -{}^t\rho\frac{\partial^t v_i}{\partial^t x_i} - ({}^t v_i - {}^t v_i^g)\frac{\partial^t \rho}{\partial^t x_i}. \tag{12}$$

EQUILIBRIUM EQUATION

Employing an incremental approach, the governing equilibrium equations for ALE must be established for the configuration at time $t + \Delta t$. The principle of virtual displacements at time $t + \Delta t$ can be written as

$$\int_{t+\Delta t V}^{t+\Delta t}\sigma_{ij}\delta_{t+\Delta t}e_{ij}^{\ t+\Delta t}dV=^{t+\Delta t}R \tag{13}$$

where $^{t+\Delta t}\sigma_{ij}$ are the components of the Cauchy stress tensor at time $t+\Delta t$ and $_{t+\Delta t}e_{ij}$ is the strain tensor defined by

$$_{t+\Delta t}e_{ij}=\frac{1}{2}(\frac{\partial u_i}{\partial^{t+\Delta t}x_j}+\frac{\partial u_j}{\partial^{t+\Delta t}x_i}) . \tag{14}$$

The external virtual work, $^{t+\Delta t}R$, is given by

$$^{t+\Delta t}R=\int_{t+\Delta t V}^{t+\Delta t}\rho^{t+\Delta t}f_i^{B}\delta u_i^{\ t+\Delta t}dV+\int_{t+\Delta t S}^{t+\Delta t}f_i^{S}\delta u_i^{\ t+\Delta t}dS \tag{15}$$

in which $^{t+\Delta t}f_i^{B}$ and $^{t+\Delta t}f_i^{S}$ are the components of the body force per unit mass and the surface traction at time $t+\Delta t$, respectively.

Since the configuration at time $t+\Delta t$ is yet unknown, an approximate solution for (13) can be obtained by referring all variables to the known grid configuration at time t and linearizing the resulting equation. In referring variables to the grid configuration, variables at time $t+\Delta t$ are assumed to be composed of their respective values at time t plus an increment given by the time derivative of the variable holding the grid point fixed multiplied by the time increment Δt. ρ Material density at time $t+\Delta t$ can be decomposed into

$$^{t+\Delta t}\rho=^{t}\rho+^{t}\rho'\Delta t \tag{16}$$

which, upon substituting with the continuity equation (12), gives

$$^{t+\Delta t}\rho=^{t}\rho-^{t}\rho\frac{\partial u_k}{\partial^{t}x_k}-(u_k-u_k^{g})\frac{\partial^{t}\rho}{\partial^{t}x_k} . \tag{17}$$

Stress components at time $t+\Delta t$ can be expressed in terms of the stresses at time t for the same grid point plus a stress increment $\sigma_{ij}'\Delta t$

$$^{t+\Delta t}\sigma_{ij}=^{t}\sigma_{ij}+^{t}\sigma_{ij}'\Delta t \tag{18}$$

and using (7), we get

$$^{t+\Delta t}\sigma_{ij}=^{t}\sigma_{ij}+^{t}\dot\sigma_{ij}\Delta t-(u_k-u_k^{g})\frac{\partial^{t}\sigma_{ij}}{\partial^{t}x_k} . \tag{19}$$

The material rate of Cauchy stresses $^{t}\dot\sigma_{ij}$ is calculated from the material constitutive relation which is usually given in terms of an objective stress rate tensor such as the Truesdell stress rate tensor defined by

$$
{}^{t}\sigma_{ij}^{T} = {}^{t}\dot{\sigma}_{ij} + \frac{\partial^{t}v_{k}}{\partial^{t}x_{k}}{}^{t}\sigma_{ij} - \frac{\partial^{t}v_{j}}{\partial^{t}x_{k}}{}^{t}\sigma_{ik} - \frac{\partial^{t}v_{i}}{\partial^{t}x_{k}}{}^{t}\sigma_{jk} . \tag{20}
$$

The material constitutive relation in terms of the Truesdell stress rate is given by

$$
{}^{t}\sigma_{ij}^{T} = {}^{t}C_{ijkl}{}^{t}D_{kl} \tag{21}
$$

where ${}^{t}D_{ij}$ is the rate of deformation tensor given by

$$
{}^{t}D_{ij} = \frac{1}{2}(\frac{\partial^{t}v_{i}}{\partial^{t}x_{j}} + \frac{\partial^{t}v_{j}}{\partial^{t}x_{i}}) \tag{22}
$$

and ${}^{t}C_{ijkl}$ is the fourth order material constitutive tensor. The variation in the strain components at time $t + \Delta t$ can be decomposed as

$$
\delta_{t+\Delta t}e_{ij} = \delta_{t}e_{ij} + \delta_{t}e_{ij}'\Delta t \tag{23}
$$

in which $\delta_{t}e_{ij}'$ is the grid time derivative of $\delta_{t}e_{ij}$ and is given by

$$
\delta_{t}e_{ij}' = -\frac{1}{2}(\frac{\partial\delta u_{i}}{\partial^{t}x_{k}}\frac{\partial^{t}v_{k}^{g}}{\partial^{t}x_{j}} + \frac{\partial\delta u_{j}}{\partial^{t}x_{k}}\frac{\partial^{t}v_{k}^{g}}{\partial^{t}x_{i}}) . \tag{24}
$$

Substitution in (23) gives

$$
\delta_{t+\Delta t}e_{ij} = \delta_{t}e_{ij} - \frac{1}{2}(\frac{\partial\delta u_{i}}{\partial^{t}x_{k}}\frac{\partial u_{k}^{g}}{\partial^{t}x_{j}} + \frac{\partial\delta u_{j}}{\partial^{t}x_{k}}\frac{\partial u_{k}^{g}}{\partial^{t}x_{i}}) . \tag{25}
$$

The body force per unit mass and traction force are incremented as

$$
{}^{t+\Delta t}f_{i}^{B} = {}^{t}f_{i}^{B} + f_{i}^{B} \tag{26}
$$

$$
{}^{t+\Delta t}f_{i}^{S} = {}^{t}f_{i}^{S} + f_{i}^{S} . \tag{27}
$$

The incremental body and traction forces f_{i}^{B} and f_{i}^{S} are assumed to be known a priori. Incremental decomposition of elemental volume at time $t + \Delta t$ in terms of the elemental volume at time t is given by

$$
{}^{t+\Delta t}dV = {}^{t}dV + {}^{t}dV'\Delta t = (1 + \frac{\partial u_{k}^{g}}{\partial^{t}x_{k}}){}^{t}dV . \tag{28}
$$

Similarly, incremental decomposition of elemental surface area is given by

$$^{t+\Delta t}dS = {}^{t}dS + {}^{t}dS'\Delta t = [1 + \frac{\partial u_k^g}{\partial^t x_k} - \frac{1}{2}(\frac{\partial u_m^g}{\partial^t x_n} + \frac{\partial u_n^g}{\partial^t x_m})^t n_m {}^t n_n]^t dS \tag{29}$$

where $^t n_m$ is the unit outward normal to the surface at time t.

Linearization is accomplished by expanding (13) using the previous incremental decompositions and neglecting higher orders in all incremental quantities. Substituting by (19), (25), and (28), the internal virtual work can be expanded, after linearization, into

$$\int_{t+\Delta t V} {}^{t+\Delta t}\sigma_{ij}\delta_{t+\Delta t}e_{ij} {}^{t+\Delta t}dV = \int_{t V} {}^t\sigma_{ij}\delta_t e_{ij} {}^t dV + \int_{t V} {}^t\dot{\sigma}_{ij}\Delta t\delta_t e_{ij} {}^t dV + \int_{t V} {}^t\sigma_{ij}\delta_t e_{ij}\frac{\partial u_k^g}{\partial^t x_k} {}^t dV$$

$$+ \int_{t V} \frac{\partial^t\sigma_{ij}}{\partial^t x_k}\delta_t e_{ij}(u_k^g - u_k)^t dV - \int_{t V} {}^t\sigma_{ij}\frac{\partial\delta u_i}{\partial^t x_k}\frac{\partial u_k^g}{\partial^t x_j} {}^t dV \tag{30}$$

The fourth integral on the RHS of (30) can be rewritten as

$$\int_{t V}\frac{\partial^t\sigma_{ij}}{\partial^t x_k}\delta_t e_{ij}(u_k^g - u_k)^t dV = \int_{t V}\frac{\partial[^t\sigma_{ij}\delta_t e_{ij}(u_k^g - u_k)]_t}{\partial^t x_k} {}^t dV - \int_{t V} {}^t\sigma_{ij}\frac{\partial\delta_t e_{ij}}{\partial^t x_k}(u_k^g - u_k)^t dV$$

$$- \int_{t V} {}^t\sigma_{ij}\delta_t e_{ij}(\frac{\partial u_k^g}{\partial^t x_k} - \frac{\partial u_k}{\partial^t x_k})^t dV \tag{31}$$

Applying the divergence theorem to the first integral in (31) and using (4)

$$\int_{t V}\frac{\partial[^t\sigma_{ij}\delta_t e_{ij}(u_k^g - u_k)]_t}{\partial^t x_k} {}^t dV = \int_{t S} {}^t\sigma_{ij}\delta_t e_{ij}(u_k^g - u_k)^t n_k {}^t dS = 0 \tag{32}$$

Substituting in (30), the internal virtual work becomes

$$\int_{t+\Delta t V} {}^{t+\Delta t}\sigma_{ij}\delta_{t+\Delta t}e_{ij} {}^{t+\Delta t}dV = \int_{t V} {}^t\sigma_{ij}\delta_t e_{ij} {}^t dV + \int_{t V} {}^t\dot{\sigma}_{ij}\Delta t\delta_t e_{ij} {}^t dV + \int_{t V} {}^t\sigma_{ij}\delta_t e_{ij}\frac{\partial u_k}{\partial^t x_k} {}^t dV$$

$$- \int_{t V} {}^t\sigma_{ij}\frac{\partial\delta_t e_{ij}}{\partial^t x_k}(u_k^g - u_k)^t dV - \int_{t V} {}^t\sigma_{ij}\frac{\partial\delta u_i}{\partial^t x_k}\frac{\partial u_k^g}{\partial^t x_j} {}^t dV \tag{33}$$

Considering the external virtual work on the RHS of (13), the body force term can be referred to the grid configuration by using (17), (26) and (28) to get

$$\int_{t+\Delta t V} {}^{t+\Delta t}\rho {}^{t+\Delta t}f_i^B\delta u_i {}^{t+\Delta t}dV = \int_{t V} {}^t\rho(^tf_i^B + f_i^B)\delta u_i {}^t dV + \int_{t V}\frac{\partial^t\rho}{\partial^t x_k} {}^tf_i^B\delta u_i(u_k^g - u_k)^t dV$$

$$+ \int_{t V} {}^t\rho{}^tf_i^B\delta u_i(\frac{\partial u_k^g}{\partial^t x_k} - \frac{\partial u_k}{\partial^t x_k})^t dV \tag{34}$$

After manipulating the second integral on the RHS of (34) in the same manner as in (31), the body force term can be rewritten as

$$\int_{t+\Delta t_V} \rho^{t+\Delta t} f_i^B \delta u_i^{t+\Delta t} dV = \int_{t_V} {}^t\rho({}^tf_i^B + f_i^B)\delta u_i^{~t} dV - \int_{t_V} {}^t\rho \frac{\partial^t f_i^B}{\partial^t x_k} \delta u_i (u_k^g - u_k)^t dV$$

$$- \int_{t_V} {}^t\rho^t f_i^B \frac{\partial \delta u_i}{\partial^t x_k}(u_k^g - u_k)^t dV \qquad (35)$$

Similarly, by using (27) and (29), the traction force term of the external virtual work can be expressed as

$$\int_{t+\Delta t_S} f_i^S \delta u_i^{~t+\Delta t} dS = \int_{t_S} ({}^tf_i^S + f_i^S)\delta u_i^{~t} dS$$

$$+ \int_{t_S} {}^tf_i^S \delta u_i [\frac{\partial u_k^g}{\partial^t x_k} - \frac{1}{2}(\frac{\partial u_m^g}{\partial^t x_n} + \frac{\partial u_n^g}{\partial^t x_m})^t n_m {}^t n_n]^t dS \qquad (36)$$

Substituting by (33), (35) and (36) into (13), the principle of virtual displacements at time $t + \Delta t$ referred to time t can be written as

$$\int_{t_V} {}^t\dot{\sigma}_{ij}\Delta t \delta_t e_{ij}^{~t} dV + \int_{t_V} {}^t\sigma_{ij}\delta_t e_{ij}\frac{\partial u_k}{\partial^t x_k}^t dV - \int_{t_V} {}^t\sigma_{ij}\frac{\partial \delta_t e_{ij}}{\partial^t x_k}(u_k^g - u_k)^t dV - \int_{t_V} {}^t\sigma_{ij}\frac{\partial \delta u_i}{\partial^t x_k}\frac{\partial u_k^g}{\partial^t x_j}^t dV$$

$$= {}^{t+\Delta t}R - \int_{t_V} {}^t\sigma_{ij}\delta_t e_{ij}^{~t} dV \qquad (37)$$

where

$$^{t+\Delta t}R = \int_{t_V} {}^t\rho({}^tf_i^B + f_i^B)\delta u_i^{~t} dV - \int_{t_V} {}^t\rho\frac{\partial^t f_i^B}{\partial^t x_k}\delta u_i(u_k^g - u_k)^t dV - \int_{t_V} {}^t\rho^t f_i^B\frac{\partial \delta u_i}{\partial^t x_k}(u_k^g - u_k)^t dV$$

$$+ \int_{t_S}({}^tf_i^S + f_i^S)\delta u_i^{~t} dS + \int_{t_S} {}^tf_i^S \delta u_i[\frac{\partial u_k^g}{\partial^t x_k} - \frac{1}{2}(\frac{\partial u_m^g}{\partial^t x_n} + \frac{\partial u_n^g}{\partial^t x_m})^t n_m {}^t n_n]^t dS \qquad (38)$$

Equation (37) represents the fully coupled ALE equation of motion. This equation can reduce to the updated Lagrangian formulation (if we choose to attach the grid to the material, i.e. $u_i^g = u_i$) and to the Eulerian formulation (if we choose to fix the grid in space, i.e. $u_i^g = 0$) as limiting cases. The constitutive relations in equations (20) to (22) can now be introduced into the third integral in (37) to give

$$\int_{t_V} {}^tC_{ijkl}\,{}_t e_{kl}\delta_t e_{ij}^{~t} dV + \int_{t_V} {}^t\sigma_{ij}\delta_t\eta_{ij}^{~t} dV$$

$$- \int_{t_V} {}^t\sigma_{ij}\frac{\partial \delta_t e_{ij}}{\partial^t x_k}(u_k^g - u_k)^t dV - \int_{t_V} {}^t\sigma_{ij}\frac{\partial \delta u_i}{\partial^t x_k}(\frac{\partial u_k^g}{\partial^t x_j} - \frac{\partial u_k}{\partial^t x_j})^t dV = {}^{t+\Delta t}R - \int_{t_V} {}^t\sigma_{ij}\delta_t e_{ij}^{~t} dV \quad (39)$$

where

$$_t\eta_{ij} = \frac{1}{2}\frac{\partial u_k}{\partial^t x_i}\frac{\partial u_k}{\partial^t x_j} \tag{40}$$

The first two integrals on the LHS of (39) are exactly the same as those obtained using an updated Lagrangian formulation. The last two integrals on the LHS are the contributions to the stiffness matrix induced by mesh motion. Thus, ALE can be considered as a logical extension to the Lagrangian formulation with simple modifications to the equation of motion of current updated Lagrangian codes. Moreover, equation (38) represents the full expression for the external virtual work with explicit terms for load correction contribution to stiffness.

Using standard finite element discretization procedure, ALE equilibrium equation (39), for an element or a group of elements, can be written in the form:

$$K_{ij}u_j + K_{ij}^g u_j^g = F_i \tag{41}$$

where K_{ij} is the tangent stiffness matrix with respect to material displacements, K_{ij}^g is the tangent stiffness matrix with respect to mesh displacements and F_i is the load vector.

DEVELOPMENT OF EULERIAN FORMULATION

In the general ALE formulation, a mesh motion scheme is used to specify the grid displacements in terms of the material displacements. Conventional finite element assembly and elimination techniques are then applied to solve for the material displacements. As indicated earlier, an Eulerian formulation can be obtained from the ALE formulation by fixing the grid in space, i.e. $u_i^g = 0$. Substitution into equation (39) yields

$$\int_{^tV} {}^tC_{ijkl}\,_t e_{kl}\delta_t e_{ij}{}^t dV + \int_{^tV} {}^t\sigma_{ij}\delta_t\eta_{ij}{}^t dV$$

$$+ \int_{^tV} {}^t\sigma_{ij}\frac{\partial\delta_t e_{ij}}{\partial^t x_k}u_k{}^t dV + \int_{^tV} {}^t\sigma_{ij}\frac{\partial\delta u_i}{\partial^t x_k}\frac{\partial u_k}{\partial^t x_j}{}^t dV = {}^{t+\Delta t}R - \int_{^tV} {}^t\sigma_{ij}\delta_t e_{ij}{}^t dV \tag{42}$$

ROLLING PROCESS SIMULATION

A steady state strip rolling process is simulated as a case study for the use of the Eulerian formulation. The pressure distribution in the rolling process is to be determined. Rolling is one of the oldest and most important forming processes. Rolling is also one of the most challenging metal forming processes in simulation because of the complexity of representation of friction and the neutral point location on the contact arc. If the Lagrangian approach is employed, mesh distortion and boundary condition updating will add to the numerical difficulties and inaccuracies of simulation. Several attempts have been made to simulate the rolling problem using the finite element method [10, 11]. In these studies, which were based on the plane strain assumption, no

comparisons were made between the computed results and experimental observations. The data for the plane strain rolling problem considered in the current work is taken similar to an experimental analysis [12] in which the contact pressure distribution was measured. The material relation is in the form

$$\sigma_{eq} = \sigma_y (1 + \frac{\varepsilon_{eq}^p}{b})^n \tag{43}$$

in which σ_{eq} is the equivalent stress, ε_{eq}^p is the equivalent plastic strain, $\sigma_y = 50.3$ MPa is the initial yield stress, $b = 0.05$ and $n = 0.26$. Young's modulus is 68.94 GPa and Poisson's ratio is 0.3. Fig. 2 shows the finite element model in which only half of the domain needs to be considered. Table 1 gives the geometric data for two different rolling configurations.

Considering the shape of the rolling pressure distribution along the arc of contact, the classical slab method always gives one pattern for the pressure distribution curve, known as the "friction hill", with maximum pressure at the neutral point, regardless of the R/h_0 ratio. However, for different rolling configurations, experiments [12, 13] showed that another pattern exists in which pressure distribution curves have double peaks with pressure drop in the middle of the arc of contact. Fig. 3 and Fig. 4 compare the experimental and computed pressure variations for the two configurations given in Table 1. Case # 1, with a relatively large R/h_0 ratio, gives a friction-hill type of distribution. Case # 2 gives a double-peak pressure distribution, which is typical for small R/h_0 ratios. It is observed that the computed results are in general agreement with the experimental ones as the two modes of pressure distributions were predicted. The discrepancies in the values of the arc of contact at the entrance and exit may be attributed to the rigid roll assumption in the finite element simulation. It is a known fact that roll flattening is an important aspect in rolling simulation which causes an increase in the arc of contact as shown in the experimental results.

Table 1. Details of the rolling process case study

Case #	Initial Height h_0 (mm)	Final Height h_1 (mm)	Radius of Roll R (mm)	R/h_0
1	2.057	1.588	79.375	39.0
2	6.274	5.385	79.375	12.5

CONCLUSIONS

In this paper, a consistent derivation of the fully coupled ALE formulation, suitable for large strain metal forming problems, is presented. The formulation is based on an incremental decomposition followed by linearization as is commonly used to derive the conventional Lagrangian formulation. The ALE formulation is shown to be a logical extension to the updated Lagrangian formulation with an arbitrary moving reference configuration and the necessary additional stiffness terms to the equilibrium equation are identified. The developed ALE formulation was implemented in a finite element program. The power of the developed formulation is that it can be reduced to both the

Lagrangian and Eulerian formulations as limiting cases. The ALE-based Eulerian formulation is successfully applied in the simulation of a rolling process. The results for the roll pressure obtained using the developed formulation compare favorably with published experimental results.

REFERENCES

[1] McMeeking, R.M. and Rice, J.R., "Finite Element Formulations for Problems of Large Elastic-Plastic Deformation", International Journal of Solids and Structures, Vol. 11, pp 601-616, (1975).

[2] Gadala, M.S., Oravas, G.A. and Dokainish, M.A., "A Consistent Eulerian Formulation of Large Deformation Problems in Statics and Dynamics", International Journal of Non-linear Mechanics, Vol. 18, No. 1, pp 21-35, (1983).

[3] Hughes, T.J.R., Liu, W.K. and Zimmermann, T.K., "Lagrangian-Eulerian Finite Element Formulation for Incompressible Viscous Flows", Computer Methods in Applied Mechanics and Engineering, Vol. 29, pp 329-349, (1981).

[4] Kennedy, J.M. and Belytschko, T.B., "Theory and Application of a Finite Element Method for Arbitrary Lagrangian-Eulerian Fluids and Structures", Nuclear Engineering and Design, Vol. 68, pp 129-146, (1981).

[5] Ghosh, S. and Kikuchi, N., "An Arbitrary Lagrangian-Eulerian Finite Element Method for Large Deformation Analysis of Elastic-Viscoplastic Solids", Computer Methods in Applied Mechanics and Engineering, Vol. 86, pp 127-188, (1991).

[6] Bayoumi, H.N., "Arbitrary Lagrangian-Eulerian Formulation For Quasi-Static And Dynamic Metal Forming Simulation", PhD Thesis, The University of British Columbia, (2001).

[7] Bayoumi, H.N. and Gadala, M.S., "A Complete Finite Element Treatment for the Fully Coupled Implicit ALE Formulation", Computational Mechanics, Vol. 33, pp 435-452, (2004).

[8] Bathe, K.J., Finite Element Procedures, Prentice-Hall, (2007).

[9] Haber, R., Shepard, M.S., Abel, J.F., Gallagher, R.H. and Greenberg, D.P., "A General Two-Dimensional, Graphical Finite Element Preprocessor Utilizing Discrete Transfinite Mappings", International Journal for Numerical Methods in Engineering, Vol. 17, pp 1015-1044, (1981).

[10] Dawson, P.R., "Viscoplastic Finite Element Analysis of Steady State Forming Processes Including Strain History and Stress Flux Dependence", Applications of Numerical Methods to Forming Processes, ASME, AMD, Vol. 28, pp 55-81, (1978).

[11] Shima, S., "Rigid Plastic Finite Element Analysis of Strip Rolling", Proceedings of the 4th International Conference on Production Engineering, pp 82-87, (1980).

[12] Al-Salehi, F.A.R., Fibrank, T.C. and Lancaster, P.R., "An Experimental Determination of the Roll Pressure distributions in Cold Rolling", International Journal for Mechanical Sciences, Vol. 15, pp 693-710, (1973).

[13] Kobayashi, S., Metal Forming and the Finite Element Method, Oxford University Press, (1989).
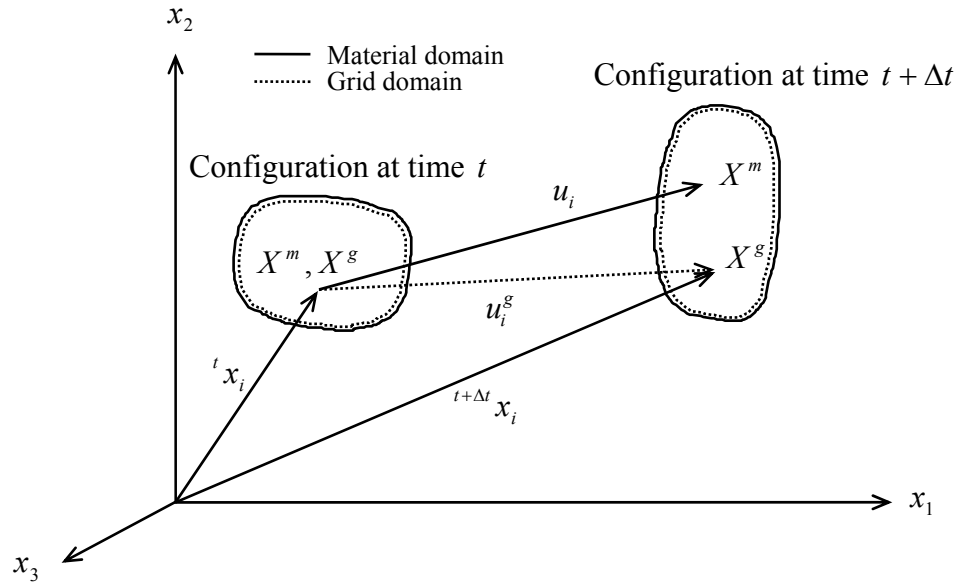
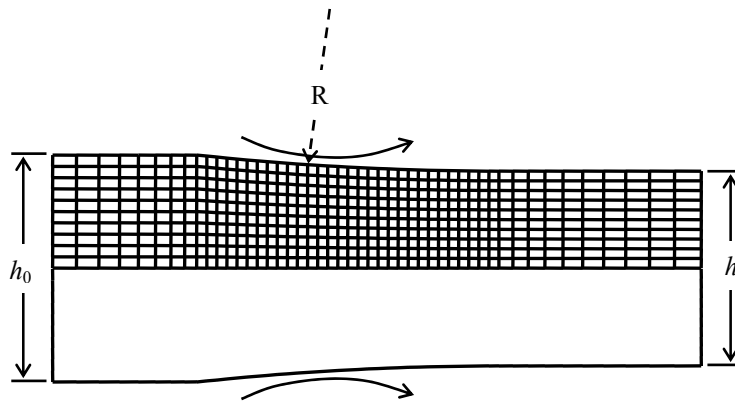Fig. 1. Description of motion

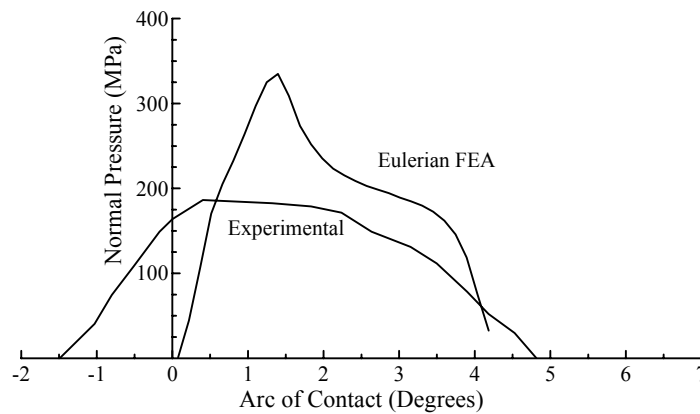
Fig 2. Geometry and mesh for rolling problem

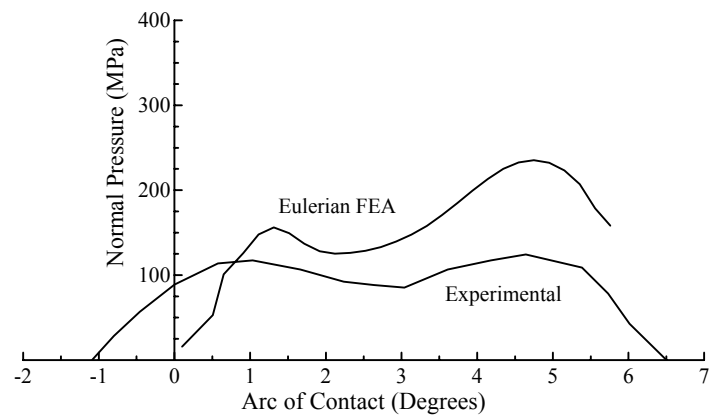Fig. 3. Comparison of roll pressure distribution for case # 1

Fig. 4. Comparison of roll pressure distribution for case # 2